Appl. Phys. A 81, 685–689 (2005)
DOI: 10.1007/s00339-005-3243-z

Applied Physics A
Materials Science & Processing

X.M. LIU
Y.C. ZHOU✉

Electrochemical deposition and characterization of Cu_2O nanowires

High-performance Ceramic Division, Shenyang National Laboratory for Materials Science,
Institute of Metal Research, Chinese Academy of Sciences, 72 Wenhua Road, Shenyang 110016, P.R. China

Received: 14 February 2005/Accepted: 23 February 2005
Published online: 20 April 2005 • © Springer-Verlag 2005

ABSTRACT Cu_2O nanowires were successfully synthesized by an electrochemical method using an alumina membrane as template through precise control of the pH value of the electrolyte. The deposition process was monitored by the time–current curve. Characterization was performed by means of X-ray diffraction, scanning electron microscopy, and transmission electron microscopy. The growth directions of the Cu_2O nanowires were determined and the possible growth mechanism is discussed.

PACS 68.37.Lp; 81.07.-b; 81.16.Be

1 Introduction

One-dimensional nanostructural materials have lately been attracting considerable attention due to their contribution to the understanding of basic concepts and potential technological applications [1]. 'Template synthesis', coined by C.R. Martin, is a versatile chemical approach for the fabrication of nanostructures [2, 3]. Recently, anodic alumina nanoporous membranes have been widely used as templates for the synthesis of nanostructures of a desired material because of their controllable pore diameters, extremely narrow size distributions for the pore diameters and their intervals, and the ideally cylindrical shape of the pores [4, 5]. The templates have been extensively used to form nanometer-size wires [6–10], rods [11], tubes [12], heterojunctions [13], and other forms of solid materials by using a variety of methods.

Cu_2O is a relatively non-toxic p-type semiconductor with a band gap of 2.1 eV [14] and is the subject of much current interest. There is evidence that Bose–Einstein condensation of excitons can occur in the material when Cu_2O is irradiated with highly intense light [15, 16]. It might be possible to transmit light through an aperture or wire with nanometer dimensions without diffraction losses [17]. Although most studies of this effect have been on large single crystals, there is interest in producing nanostructures of Cu_2O, because it may be possible to observe condensation of excitons at a lower intensity of light. Water-splitting activity has been reported in a vigorously stirred, illuminated suspension of Cu_2O particles, although the exact mechanism and precise role of the oxide are unclear [18, 19]. Recently, it has been found that Cu_2O submicrospheres can be used as a negative-electrode material for lithium-ion batteries [20].

Electrochemical deposition (ED) could be a convenient way of engineering the crystal orientations of semiconducting films or nanowires. Highly textured semiconductor films or nanowires, for example Cu_2O [21–26] and Bi_2Ti_3 [9, 10, 27], have been electrochemically prepared. Epitaxial electrodeposition has also been made on single-crystal copper and gold [28, 29]. There are already several papers on the synthesis of Cu_2O nanowires using different methods [26, 30–33]. But, the products reported in the literature were, however, sometimes characterized by relatively low yields [32], polycrystallinity [30, 31], and low aspect ratios [30, 32]. Thus, methods need to be developed to overcome these problems.

Here, we report the electrochemical deposition of Cu_2O nanowires using an alumina membrane (AM) as template. This method, combining the advantage of the AM template synthesis with electrochemical deposition (low temperature and low cost), is competitive to other methods.

2 Experimental

Alumina membranes with an average diameter of 100 nm were used (Whatman Anodisc 25). The membranes have a pore density of $\sim 10^9$ (pores/cm^2), a mean porosity of 30%, and a thickness of 60 μm.

The electrochemical deposition of Cu_2O nanowires into the membrane was conducted in an electrolyte solution consisting of 0.4 M cupric sulfate and 3 M lactic acid. By complexing with lactate ion, the copper was stabilized and the pH could be raised to alkaline values. The pH of the solution was adjusted to 8.0 by the addition of 5 M NaOH and the solution was stirred overnight. Before use, a small amount of NaOH was added to further adjust the pH value of the electrolyte. The solution temperature was kept at 60 °C during the whole experiment. Electrochemical deposition and examinations were performed in a flat cell (EG&G PARC) with a CHI 660A electrochemical workstation (CH Instruments, Inc., USA) under computer control. The working electrode was constructed as follows. First, a layer of gold with a thickness of about 100 nm was evaporated on to one side of the membrane. Second, an in-

✉ Fax: +86-24-238-913-20, E-mail: yczhou@imr.ac.cn

dium tin oxide (ITO) electrode was used as a current collector and contacted to the gold layer on the one side of the membrane. These two parts were fixed between the hole and the steel slide of the flat cell, with the bare side of the membrane ($\sim 0.5\ \mathrm{cm}^2$) facing the electrolyte. The counter electrode was a round piece of copper foil (diameter 6 cm). The reference electrode was a saturated calomel electrode (SCE).

Phase identification was performed by means of X-ray diffraction (XRD) using a D/max-2500 PC X-ray diffractometer (Rigaku, Japan) with Cu K_α radiation. The samples for XRD analysis were made by mechanically polishing away the overgrowth layer on the AM. For scanning electron microscopy (SEM) observation, Cu_2O nanowires/AM composites were fixed to a piece of double-sided, conducting adhesive tape and dipped in 2 M aqueous NaOH for different times to dissolve the AM. After being carefully rinsed with deionized water several times and dried in air, the tape was attached to a carbon stub and a thin layer of gold (~ 5 nm) was sputtered on to the samples. The samples were examined in a S-360 scanning electron microscope (Cambridge Instruments, UK) equipped with a LINK ISIS 300 energy-dispersive spectroscopy (EDS) system (Oxford Instruments, UK). For transmission electron microscopy (TEM) investigations, the products were immersed in 2 M aqueous NaOH for 30 min at room temperature to dissolve the AM. The samples were filtrated by a 20-nm track-etched polycarbonate membrane (Whatman International Ltd., UK) and were then washed with distilled water several times. After dispersing in alcohol by ultrasonic vibration for two minutes, a small drop of the solution containing the nanowires was dropped on to a Cu grid covered with a carbon film and dried in air. Low-magnification images were taken with a Philips EM-420 TEM. High-resolution TEM (HRTEM) observations were performed in a JEOL-2010 microscope operating at 200 kV.

3 Results

First, the potential for electrochemical deposition must be determined. A cyclic voltammogram using a gold-evaporated AM as template shows that a potential window between -0.4 V and -0.6 V (vs. SCE) can be used to deposit Cu_2O nanowires. But, at a more negative potential, the current will increase and copper will be codeposited with Cu_2O, so a potential of -0.45 V was used in all experiments. It is also confirmed that Cu_2O nanowires can be deposited at a reasonable rate at -0.45 V.

The deposition process was monitored by the time–current (t–J) curve [4]. The change of current density (J) during the electrochemical reaction at a constant applied potential of -0.45 V is shown in Fig. 1. Since the deposition current depends on the mass-transport conditions and the effective surface area of the electrode, the recorded t–J curve during Cu_2O deposition reveals four different stages. (1) Initially, the electrochemical reaction takes place at the substrate/electrolyte interface and a large amount of nuclei forms. During this process the current density decreases rapidly due to the limited mass transport and the semiconducting nature of the product. (2) Cu_2O grows inside the pores of the AM and the current density first decreases slightly and then increases slightly; this may be caused by the diffusion of the electrolyte. At the beginning of the deposition, the diffusion distance between the electrolyte and the reaction tip is long, and the current density decreases slightly. As the distance becomes shorter and once it reaches a certain value, a slight increase in the current density is observed. (3) The pores are filled with Cu_2O to the top and, at the membrane surface, cap formation associated with three-dimensional deposition is observed. Thus, the effective cathode area increases and a rapid increase of the deposition current density can be observed. (4) Thereafter, the hemispherical caps originating from each nanowire form a coherent, planar layer that expands until it covers the entire surface of the membrane and the effective surface area reaches a constant value, which accompanies a steady current density. Note that the steady current density of stage (4) is about three times that of stage (2), which is consistent with the mean porosity (30%) of the AM. For the present study,

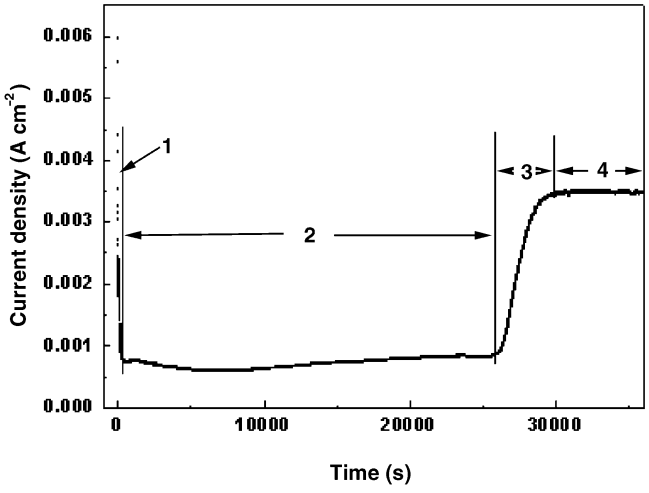

FIGURE 1 Time–current density curve showing different stages of the pore-filling process during the electrochemical deposition of Cu_2O. 1: Nuclei formation on the evaporated Au film; 2: Cu_2O nanowire deposition in the pores of the AM; 3: three-dimensional hemispherical cap formation; 4: Cu_2O film formation on the AM surface

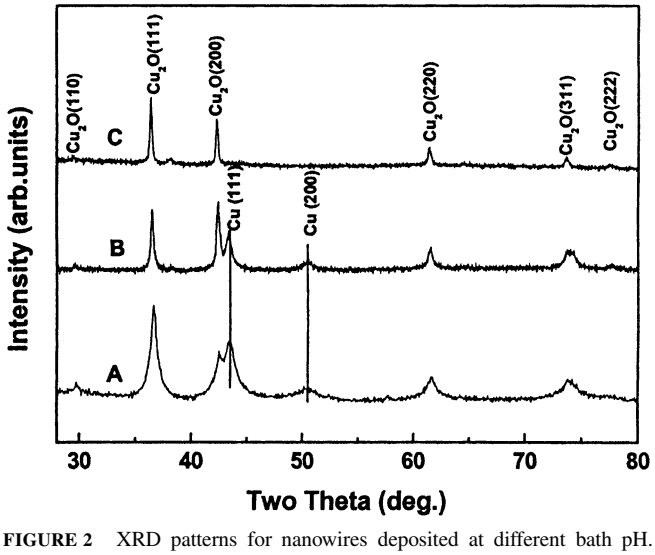

FIGURE 2 XRD patterns for nanowires deposited at different bath pH. The applied potential is -0.45 V (vs. SCE). A: pH = 8.0, B: pH = 8.3, C: pH = 8.6

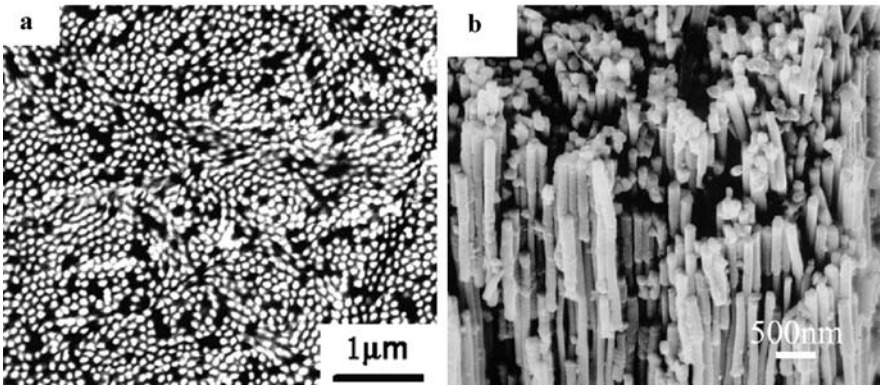

FIGURE 3 (**a**) SEM surface view of Cu_2O nanowire array, (**b**) SEM image after part of the AM has been dissolved

the electrodeposition process was stopped between stage (2) and stage (3), when a rapid increase in current density was observed.

As a low pH value is favorable for the stability of the AM (the pH range is from 4 to 8 [34]), we tried to deposit Cu_2O nanowires at lower pH values. It has been reported that a Cu_2O film can be deposited at a pH value as low as 8.0 [25]. So, the deposition of Cu_2O nanowires was first tried using a pH value of 8.0. Figure 2 shows the XRD patterns of nanowires deposited at different pH values. The nanowires deposited at pH = 8.0 (curve A) are a composite of Cu_2O and Cu, and the strong peak broadening observed is interpreted by the small grain size of the composite, which is confirmed by the result of electron diffraction (not shown). In the sample prepared at a pH value of 8.3 (curve B), there are still peaks of Cu, but the intensities are much lower than those deposited at pH = 8.0, which means that less Cu is deposited under a little higher pH value. In the sample deposited at the electrolyte pH value of 8.6, no reflections from Cu can be detected, as is shown in curve C. All the diffraction peaks in curve C can be indexed as cuprite phase of Cu_2O, i.e. pure Cu_2O nanowires are obtained. This condition was selected as the standard procedure to deposit Cu_2O nanowires, and subsequent SEM and TEM characterizations were done on samples deposited under the same condition.

Figure 3a shows a typical SEM surface view of a Cu_2O nanowire array after briefly polishing off the overgrowth layer. It has been calculated that the pore-filling rate has reached about 80%. This high pore-filling rate may have some relation with the deposition condition used in this work. The low pH value and the low voltage used make the deposition rate slow. In another words, the condition is closer to equilibrium. So, the deposition can proceed homogeneously. Figure 3b shows a typical SEM image of a Cu_2O nanowire array after the AM has been partly etched away by 2 M NaOH. It can be seen that the product has a high wire density. The tip of each nanowire is flat and all the nanowires have almost the same height, indicating that the nanowires are deposited homogeneously. The nanowires have high aspect ratio (more than 300 in this sample), as can be seen after etching away nearly all the AM. Energy-dispersive spectroscopy (EDS) also confirms that the nanowires are composed of Cu and O with the atomic ratio of about 2:1.

A conventional TEM image of Cu_2O nanowires is shown in Fig. 4a. The figure shows that they have almost the same diameter, indicating the uniformity of the product. The measured diameters (about 130 nm) of the Cu_2O nanowires correspond satisfactorily to the pore size of the AM used[1], which also indicates that the pores of the AM were not etched by the electrolyte during deposition. Some short and sharp end wires can also be found, which may be caused during ultrasonic vibration used to prepare the TEM samples. We have characterized some samples made in similar conditions by XRD and TEM, and found that the reproducibility of the method is good. The nanowires produced by the method can have different aspect ratios, which are determined by the deposition time used. An aspect ratio as large as 600 can be expected, as the nominal thickness and diameter are 60 μm and 100 nm, respectively. Cu_2O nanowires deposited for a short time will have a low aspect ratio. Figure 4b shows a TEM image of a typical Cu_2O nanowire deposited at a pH value of 8.6 and its selected area electron diffraction (SAED) pattern (inset). The SAED patterns taken from different parts of the nanowire are exactly the same without further tilting the nanowire, which indicates the single crystallinity of the nanowire. Several tens of individual nanowires have been examined using this method in the same sample, and the diffraction patterns suggest that all of them grow either along the ⟨001⟩ direction or the ⟨110⟩ direction, as shown in Fig. 4b and 4d. The high-resolution TEM images taken from different nanowires shown in Fig. 4c and 4e further confirm that they grow along the ⟨001⟩ or the ⟨110⟩ direction. The XRD result shown in Fig. 2 also confirms this conclusion. We have calculated the intensities ratio of (200) and (110) peaks to that of (111). The results are 68% and 20%, respectively. These values are higher than those in JCPDS (05-0667, 37% and 9% respectively), implying that the product has some degree of preferred orientation. The sample for XRD characterization has had the overgrowth layer on the AM briefly mechanically ground away, which may lower the intensity ratio.

4 Discussion

It can be seen from the XRD and SAED results (not shown here) that the lowest pH value for pure Cu_2O nanowire deposition is a little higher than that for a Cu_2O film (8.6 vs. 8.0) [25]. Cu would codeposit with Cu_2O at a low pH value (smaller than 8.6). This might be explained by the reaction

[1] The quoted pore diameter of the AM is 100 nm but, actually, according to the SEM image of the AM, there is a pore-diameter distribution mainly in the range of 110–150 nm.

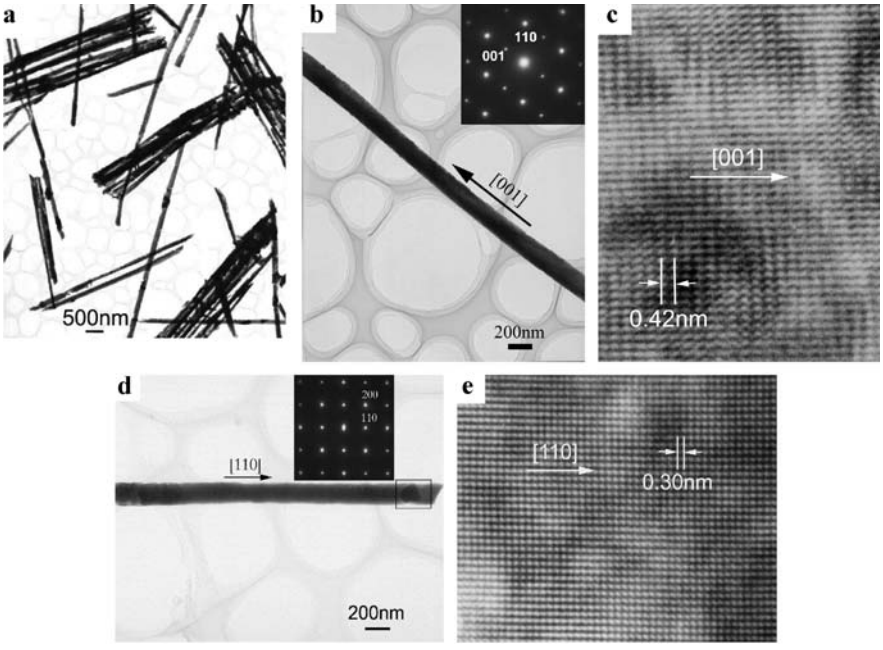

FIGURE 4 TEM and HRTEM images of Cu_2O nanowires showing their morphologies and growth directions. (**a**) Typical TEM images of Cu_2O nanowires showing uniform diameter of about 130 nm. (**b**) A TEM image of a single Cu_2O nanowire deposited at a pH value of 8.6. The *inset* is the SAED pattern recorded along the $[1\bar{1}0]$ zone axis. (**c**) HRTEM image taken from the edge of the same nanowire shown in (**b**). (**d**) A TEM image and its corresponding SAED pattern of a single Cu_2O nanowire showing the $\langle 110 \rangle$ growth direction. The incident electron beam is along the [001] zone axis. (**e**) HRTEM image taken from the box in (**d**) (which may be caused by ultrasonic vibration)

mechanism of the system and the nanochannel feature of the AM.

The reactions for preparing Cu_2O can be expressed as follows:

$$2\,Cu^{2+} + 2\,e + 2OH^- \rightarrow 2\,CuOH \rightarrow Cu_2O + H_2O. \quad (1)$$

During the electrochemical deposition, OH^- is consumed and the diffusion of it from bulk electrolyte through the narrow channels of the AM to the front tip of the reaction is more difficult than that for the case of deposition of a Cu_2O film, which may cause the decrease of the pH value at the reaction interface. Then, reduction of Cu^{2+} to metallic copper will occur:

$$Cu^{2+} + 2\,e \rightarrow Cu. \quad (2)$$

The slow diffusion rate of OH^- may be the reason why the pH value for the deposition of Cu_2O nanowires in the AM is higher than that for the deposition of a Cu_2O film on a flat substrate. It is also found that, even after putting the AM in the electrolyte at pH = 8.6 for 10 h, the membrane is only slightly dissolved, indicating that this pH value is suitable for electrochemical synthesis of Cu_2O nanowires.

It is interesting that Cu_2O nanowires have $\langle 001 \rangle$ and $\langle 110 \rangle$ growth directions, which is different from the orientation of an electrochemically deposited Cu_2O film. Under similar conditions, only the $\langle 001 \rangle$ preferred orientation can be observed for a Cu_2O film [14, 25], while a high pH value (pH = 11 [14]) and a high voltage [21] are favorable for the [111] and [311] preferred orientations, respectively. These conditions, which are far from equilibrium, are very different from the condition used in this paper. So, we do not expect to observe these growth directions of the nanowires. The growth direction of Cu_2O is related to the polarity of different planes. The $\{111\}$ plane is a non-polar surface. However, in planes that are parallel to $\{001\}$ surfaces, copper- and oxygen-containing planes alternate, which results in a dipole across the crystal. The $\{001\}$ surface of Cu_2O is unstable and the net dipole over the crystal must be eliminated to generate a stable surface. If the O^{2-} ions are exposed in the $\{001\}$ surface, converting the O^{2-} anions at the surface to OH^- leads to the required stabilization. Therefore, the O^{2-} ions in the $\{001\}$ surface are more apt to hydrolyze, compared with those in the $\{111\}$ surface. The stacking along the $\langle 001 \rangle$ direction therefore becomes energetically favorable. This is the reason why the fibers, known as chalcotrichite, greatly elongate along the $\langle 001 \rangle$ direction [35]. The result that there is no $\langle 111 \rangle$ growth direction is also consistent with the film orientation that forms at this pH value [14, 25]. The existence of the $\langle 110 \rangle$ growth direction may be related to the growth rate of different crystallographic planes of the Cu_2O crystal. The $\{110\}$ plane is one of the close-packed planes of Cu_2O. These planes have lower surface energy, so that the growth rate on them will be faster than that on the $\{111\}$ plane. This may be the reason why some Cu_2O nanowires grow along the $\langle 110 \rangle$ direction. In the work of Oh et al. [26], no $\langle 110 \rangle$ growth direction was observed. This may be caused by the difference of deposition conditions. In this work the deposition is carried out at a constant-voltage condition. It can be seen from Fig. 1 that the steady current is about twice that of Oh et al.'s work ($0.5\,mA\,cm^{-2}$) [26]. In other words, the condition used is very far away from equilibrium. That is why the less energy favorable [110] growth direction can occur in this study.

5 Conclusion

In summary, electrochemical deposition of Cu_2O nanowires using an AM as template was studied. The result shows that, by precisely controlling the pH value of the electrolyte, pure Cu_2O nanowires can be formed in the AM. The aspect ratio of the nanowires can be controlled through varying the deposition time. The nanowires are uniform arrays of single crystals, which grow along $\langle 001 \rangle$

and ⟨110⟩ directions. The growth directions of the Cu_2O nanowires are explained from the surface-energy point of view.

ACKNOWLEDGEMENTS This work was financially supported by the National Outstanding Young Scientist Foundation for Y.C. Zhou under Grant No. 59 925 208 and the National Science Foundation of China under Grant Nos. 50 072 034 and 59 772 021.

REFERENCES

1 C.M. Lieber: Solid State Commun. **107**, 607 (1998)
2 C.R. Martin: Science **266**, 1961 (1994)
3 J.C. Hulteen, C.R. Martin: J. Mater. Chem. **7**, 1075 (1997)
4 T.M. Whitney, J.S. Jiang, P.C. Searson, C.L. Chien: Science **261**, 1316 (1993)
5 H. Masuda, K. Fukuda: Science **268**, 1466 (1995)
6 M.S. Sander, A.L. Prieto, R. Gronsky, T. Sands, A.M. Stacy: Adv. Mater. **14**, 665 (2002)
7 M.J. Zheng, G.H. Li, X.Y. Zhang, S.Y. Huang, Y. Lei, L.D. Zhang: Chem. Mater. **13**, 3859 (2001)
8 J.C. Bao, D.P. Xu, Q.F. Zhou, Z. Xu: Chem. Mater. **14**, 4709 (2002)
9 C.G. Jin, X.Q. Xiong, W.F. Liu, W.L. Cai, L.Z. Yao, X.G. Li: J. Phys. Chem. B **108**, 1844 (2004)
10 M.S. Sander, R. Gronsky, T. Sands, A.M. Stacy: Chem. Mater. **15**, 335 (2001)
11 B.R. Martin, D.J. Dermody, B.D. Reiss, M.M. Fang, L.A. Lyon, M.J. Natan, T.E. Mallouk: Adv. Mater. **11**, 1021 (1999)
12 J. Sha, J.J. Niu, X.Y. Ma, J. Xu, X.B. Zhang, Q. Yang, D. Yang: Adv. Mater. **14**, 1219 (2002)
13 J. Luo, L. Zhang, Y.J. Zhang, J. Zhu: Adv. Mater. **14**, 1413 (2002)
14 T.D. Golden, M.G. Shumsky, Y.C. Zhou, R.A. VanderWerf, R.A. Van Leeuwen, J.A. Switzer: Chem. Mater. **8**, 2499 (1996)
15 A. Mysyrowicz, E. Benson, E. Fortin: Phys. Rev. Lett. **77**, 896 (1996)
16 K. Johnsen, G.M. Kavoulakis: Phys. Rev. Lett. **86**, 858 (2001)
17 D. Snoke: Science **273**, 1351 (1996)
18 P.E. de Jongh, D. Vanmaekelbergh, J.J. Kelly: Chem. Commun. 1069 (1999)
19 M. Hara, T. Kondo, M. Komoda, S. Ikeda, K. Shinohara, A. Tanaka, J.N. Kondo, K. Domen: Chem. Commun. 357 (1998)
20 P. Poizot, S. Laruelle, S. Grugeon, L. Dupont, J.M. Tarascon: Nature **407**, 496 (2000)
21 T. Mahalingam, J.S.P. Chitra, S. Rajendran, P.J. Sebastian: Semicond. Sci. Technol. **17**, 565 (2002)
22 D. Tench, L.E. Warren: J. Electrochem. Soc. **130**, 869 (1983)
23 A.E. Rakhshani, J. Varghese: Thin Solid Films **157**, 87 (1988)
24 A.P. Chatterjee, A.K. Mukhopadhyay, A.K. Chakraborty, R.N. Sasmal, S.K. Lahiri: Mater. Lett. **11**, 358 (1991)
25 Y.C. Zhou, J.A. Switzer: Scr. Mater. **38**, 1731 (1998)
26 J. Oh, Y. Tak, Y. Lee: Electrochem. Solid State Lett. **7**, C27 (2004)
27 Y. Miyazaki, T. Kajitani: J. Cryst. Growth **229**, 542 (2001)
28 J.K. Barton, A.A. Vertegel, E.W. Bohannan, J.A. Switzer: Chem. Mater. **13**, 952 (2001)
29 E.W. Bohannan, M.G. Shumsky, J.A. Switzer: Chem. Mater. **11**, 2289 (1999)
30 Y.J. Xiong, Z.Q. Li, R. Zhang, Y. Xie, J. Yang, C.Z. Wu: J. Phys. Chem. B **107**, 3697 (2003)
31 S.H. Wang, Q.J. Huang, X.G. Wen, X.Y. Li, S.H. Yang: Phys. Chem. Chem. Phys. **4**, 3425 (2002)
32 L.M. Huang, H.T. Wang, Z.B. Wang, A.P. Mitra, D. Zhao, Y.H. Yan: Chem. Mater. **14**, 876 (2002)
33 W.Z. Wang, G.H. Wang, X.S. Wang, Y.J. Zhan, Y.K. Liu, C.L. Zheng: Adv. Mater. **14**, 67 (2002)
34 P.P. Mardilovich, A.N. Govyadinov, N.I. Mazurenko, R. Paterson: J. Membrane Sci. **98**, 143 (1995)
35 L.G. Berry, B. Mason: *Mineralogy: Concepts, Descriptions, Determinations* (Freeman, San Francisco, CA 1959)